

Precise ATLAS and CMS DY data in the ABM fit

S.Alekhin (*Univ. of Hamburg & IHEP Protvino*)

(in collaboration with J.Blümlein and S.Moch)

DY data in ABMP16 fit

TABLE II. The list of DIS and DY data used in the current analysis with the collider data listed first. The top-quark production data are detailed in Tables III and IV.

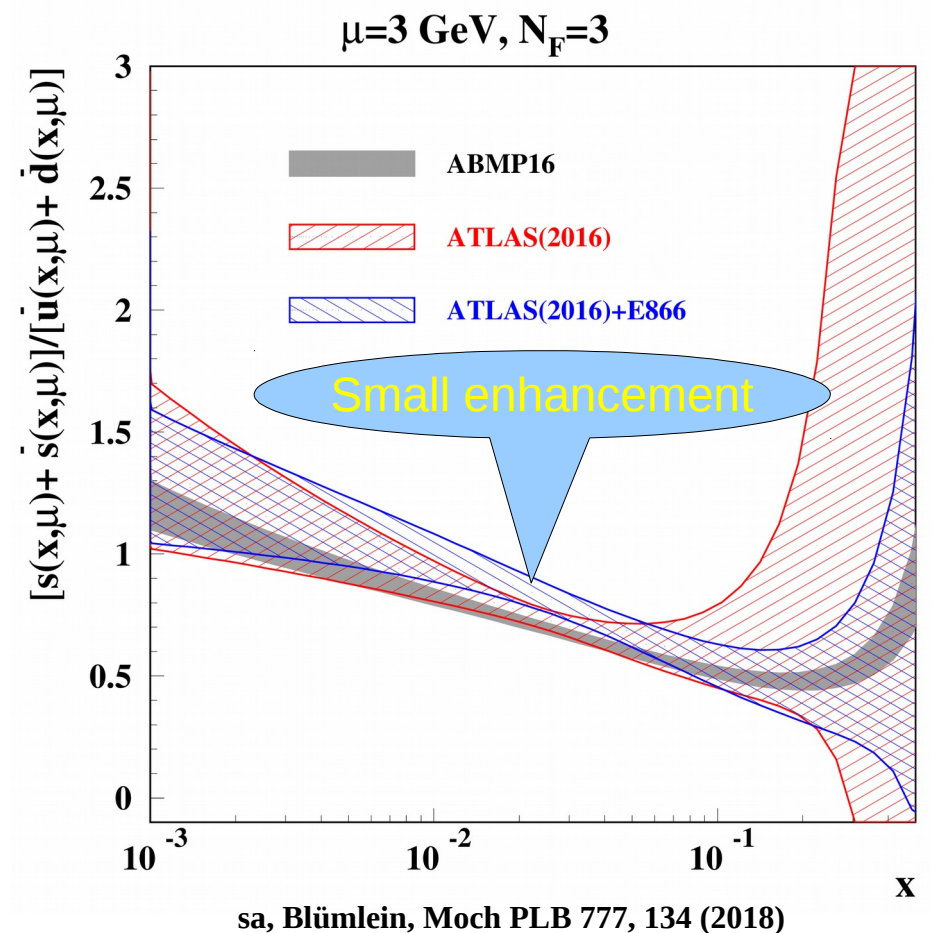
Experiment	Beam (E_b) or center-of-mass energy (\sqrt{s})	\mathcal{L} (1/fb)	Process	Kinematic cuts used in the present analysis (cf. original references for notations)	Ref.
<i>DIS</i>					
HERA I + II	$\sqrt{s} = 0.225 \div 0.32$ TeV	0.5	$e^\pm p \rightarrow e^\pm X$ $e^\pm p \rightarrow \bar{\nu} X$	$2.5 \leq Q^2 \leq 50000 \text{ GeV}^2$, $2.5 \times 10^{-5} \leq x \leq 0.65$ $200 \leq Q^2 \leq 50000 \text{ GeV}^2$, $1.3 \times 10^{-2} \leq x \leq 0.40$	[4]
BCDMS	$E_b = 100 \div 280 \text{ GeV}$		$\mu^+ p \rightarrow \mu^+ X$	$7 < Q^2 < 230 \text{ GeV}^2$, $0.07 \leq x \leq 0.75$	[61]
NMC	$E_b = 90 \div 280 \text{ GeV}$		$\mu^+ p \rightarrow \mu^+ X$	$2.5 \leq Q^2 < 65 \text{ GeV}^2$, $0.009 \leq x < 0.5$	[60]
SLAC-49a	$E_b = 7 \div 20 \text{ GeV}$		$e^- p \rightarrow e^- X$	$2.5 \leq Q^2 < 8 \text{ GeV}^2$, $0.1 < x < 0.8$, $W \geq 1.8 \text{ GeV}$	[54]
SLAC-49b	$E_b = 4.5 \div 18 \text{ GeV}$		$e^- p \rightarrow e^- X$	$2.5 \leq Q^2 < 20 \text{ GeV}^2$, $0.1 < x < 0.9$, $W \geq 1.8 \text{ GeV}$	[62]
SLAC-87	$E_b = 8.7 \div 20 \text{ GeV}$		$e^- p \rightarrow e^- X$	$2.5 \leq Q^2 < 20 \text{ GeV}^2$, $0.3 < x < 0.9$, $W \geq 1.8 \text{ GeV}$	[54]
SLAC-89b	$E_b = 6.5 \div 19.5 \text{ GeV}$		$e^- p \rightarrow e^- X$	$2.5 \leq Q^2 \leq 19 \text{ GeV}^2$, $0.17 < x < 0.9$, $W \geq 1.8 \text{ GeV}$	[56]
<i>DIS heavy-quark production</i>					
HERA I + II	$\sqrt{s} = 0.32 \text{ TeV}$		$e^\pm p \rightarrow e^\pm cX$	$2.5 \leq Q^2 \leq 2000 \text{ GeV}^2$, $2.5 \times 10^{-5} \leq x \leq 0.05$	[63]
H1	$\sqrt{s} = 0.32 \text{ TeV}$	0.189	$e^\pm p \rightarrow e^\pm bX$	$5 \leq Q^2 \leq 2000 \text{ GeV}^2$, $2 \times 10^{-4} \leq x \leq 0.05$	[15]
ZEUS	$\sqrt{s} = 0.32 \text{ TeV}$	0.354	$e^\pm p \rightarrow e^\pm bX$	$6.5 \leq Q^2 \leq 600 \text{ GeV}^2$, $1.5 \times 10^{-4} \leq x \leq 0.035$	[16]
CCFR	$87 \lesssim E_b \lesssim 333 \text{ GeV}$		$\bar{\nu} N \rightarrow \mu^\pm cX$	$1 \leq Q^2 < 170 \text{ GeV}^2$, $0.015 \leq x \leq 0.33$	[64]
CHORUS	$\langle E_b \rangle \approx 27 \text{ GeV}$		$\nu N \rightarrow \mu^+ cX$		[18]
NOMAD	$6 \leq E_b \leq 300 \text{ GeV}$		$\nu N \rightarrow \mu^+ cX$	$1 \leq Q^2 < 20 \text{ GeV}^2$, $0.02 \lesssim x \leq 0.75$	[17]
NuTeV	$79 \lesssim E_b \lesssim 245 \text{ GeV}$		$\bar{\nu} N \rightarrow \mu^\pm cX$	$1 \leq Q^2 < 120 \text{ GeV}^2$, $0.015 \leq x \leq 0.33$	[64]
<i>DY</i>					
ATLAS	$\sqrt{s} = 7 \text{ TeV}$	0.035	$pp \rightarrow W^\pm X \rightarrow l^\pm \nu X$	$p_T^l > 20 \text{ GeV}$, $p_T^\nu > 25 \text{ GeV}$, $m_T > 40 \text{ GeV}$	[67]
	$\sqrt{s} = 13 \text{ TeV}$	0.081	$pp \rightarrow ZX \rightarrow l^+ l^- X$ $pp \rightarrow W^\pm X \rightarrow l^\pm \nu X$ $pp \rightarrow ZX \rightarrow l^+ l^- X$	$p_T^l > 20 \text{ GeV}$, $66 < m_{ll} < 116 \text{ GeV}$ $p_T^\nu > 25 \text{ GeV}$, $m_T > 50 \text{ GeV}$ $p_T^l > 25 \text{ GeV}$, $66 < m_{ll} < 116 \text{ GeV}$	[26]
CMS	$\sqrt{s} = 7 \text{ TeV}$	4.7	$pp \rightarrow W^\pm X \rightarrow \mu^\pm \nu X$	$p_T^\mu > 25 \text{ GeV}$	[24]
	$\sqrt{s} = 8 \text{ TeV}$	18.8	$pp \rightarrow W^\pm X \rightarrow \mu^\pm \nu X$	$p_T^\mu > 25 \text{ GeV}$	[25]
DØ	$\sqrt{s} = 1.96 \text{ TeV}$	7.3	$\bar{p}p \rightarrow W^\pm X \rightarrow \mu^\pm \nu X$	$p_T^\mu > 25 \text{ GeV}$, $E_T > 25 \text{ GeV}$	[23]
		9.7	$\bar{p}p \rightarrow W^\pm X \rightarrow e^\pm \nu X$	$p_T^e > 25 \text{ GeV}$, $E_T > 25 \text{ GeV}$	[22]
LHCb	$\sqrt{s} = 7 \text{ TeV}$	1	$pp \rightarrow W^\pm X \rightarrow \mu^\pm \nu X$	$p_T^\mu > 20 \text{ GeV}$	[19]
	$\sqrt{s} = 8 \text{ TeV}$	2	$pp \rightarrow ZX \rightarrow \mu^+ \mu^- X$	$p_T^\mu > 20 \text{ GeV}$, $60 < m_{\mu\mu} < 120 \text{ GeV}$	[21]
		2.9	$pp \rightarrow ZX \rightarrow e^+ e^- X$ $pp \rightarrow W^\pm X \rightarrow \mu^\pm \nu X$ $pp \rightarrow ZX \rightarrow \mu^+ \mu^- X$	$p_T^e > 20 \text{ GeV}$, $60 < m_{ee} < 120 \text{ GeV}$ $p_T^\mu > 20 \text{ GeV}$ $p_T^\mu > 20 \text{ GeV}$, $60 < m_{\mu\mu} < 120 \text{ GeV}$	[20]
FNAL-605	$E_b = 800 \text{ GeV}$		$pCu \rightarrow \mu^+ \mu^- X$	$l \leq M_{\mu\mu} \leq 18 \text{ GeV}$	[68]
FNAL-866	$E_b = 800 \text{ GeV}$		$pp \rightarrow \mu^+ \mu^- X$ $pD \rightarrow \mu^+ \mu^- X$	$4.6 \leq M_{\mu\mu} \leq 12.9 \text{ GeV}$	[69]

Impact of ATLAS data on strangeness

	$\kappa_s(\mu^2=20 \text{ GeV}^2)$
HERA+ATLAS	0.81(18)
HERA+ATLAS+E866	0.72(8)
ABMP16(incl. NOMAD)	0.66(3)

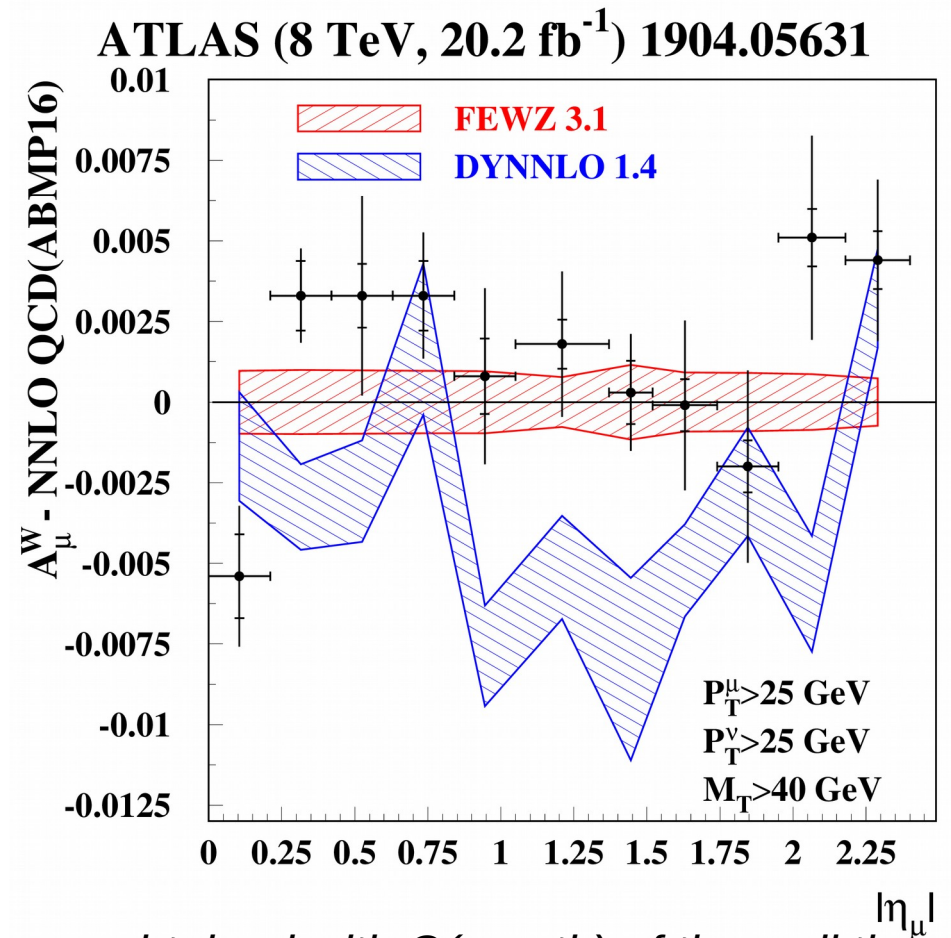
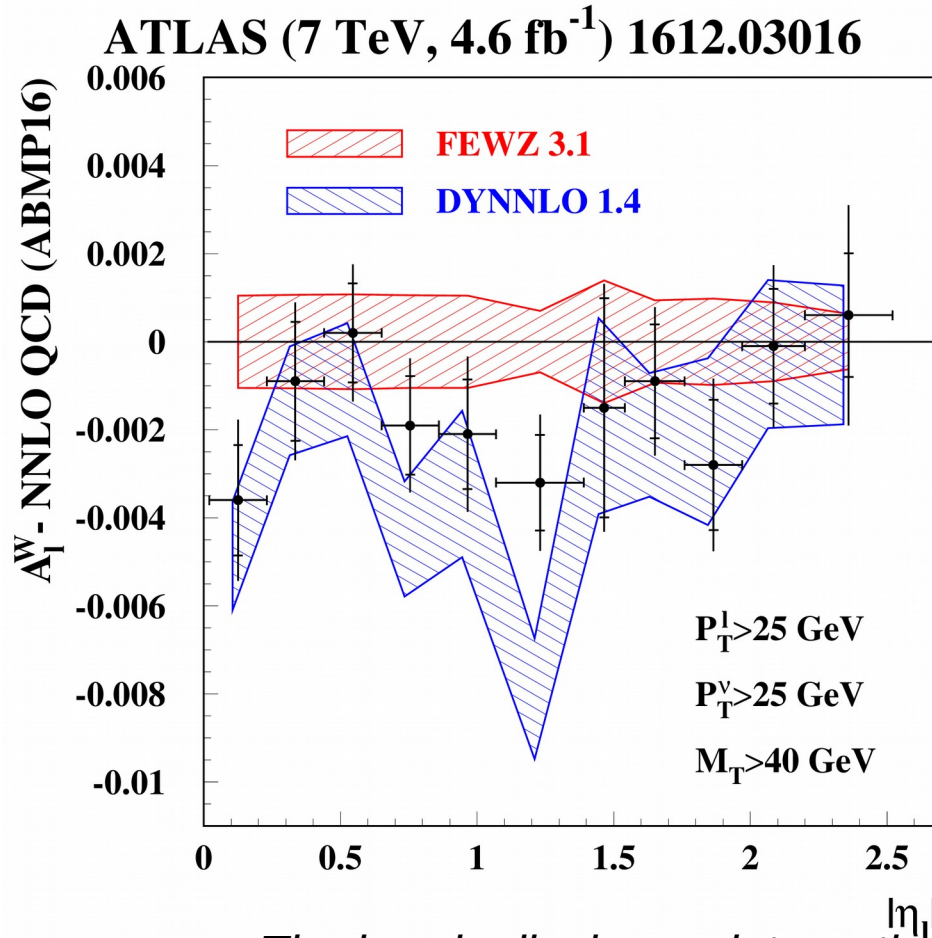
κ_s is integral strange sea suppression factor:

$$\kappa_s(\mu^2) = \frac{\int_0^1 x[s(x, \mu^2) + \bar{s}(x, \mu^2)]dx}{\int_0^1 x[\bar{u}(x, \mu^2) + \bar{d}(x, \mu^2)]dx},$$



- The strangeness is in a broad agreement with the one extracted from the dimuon data
- The E866 data are consistent with the ATLAS(2016) central data:
 $\chi^2/\text{NDP}=48/39$ and $40/34$, respectively.

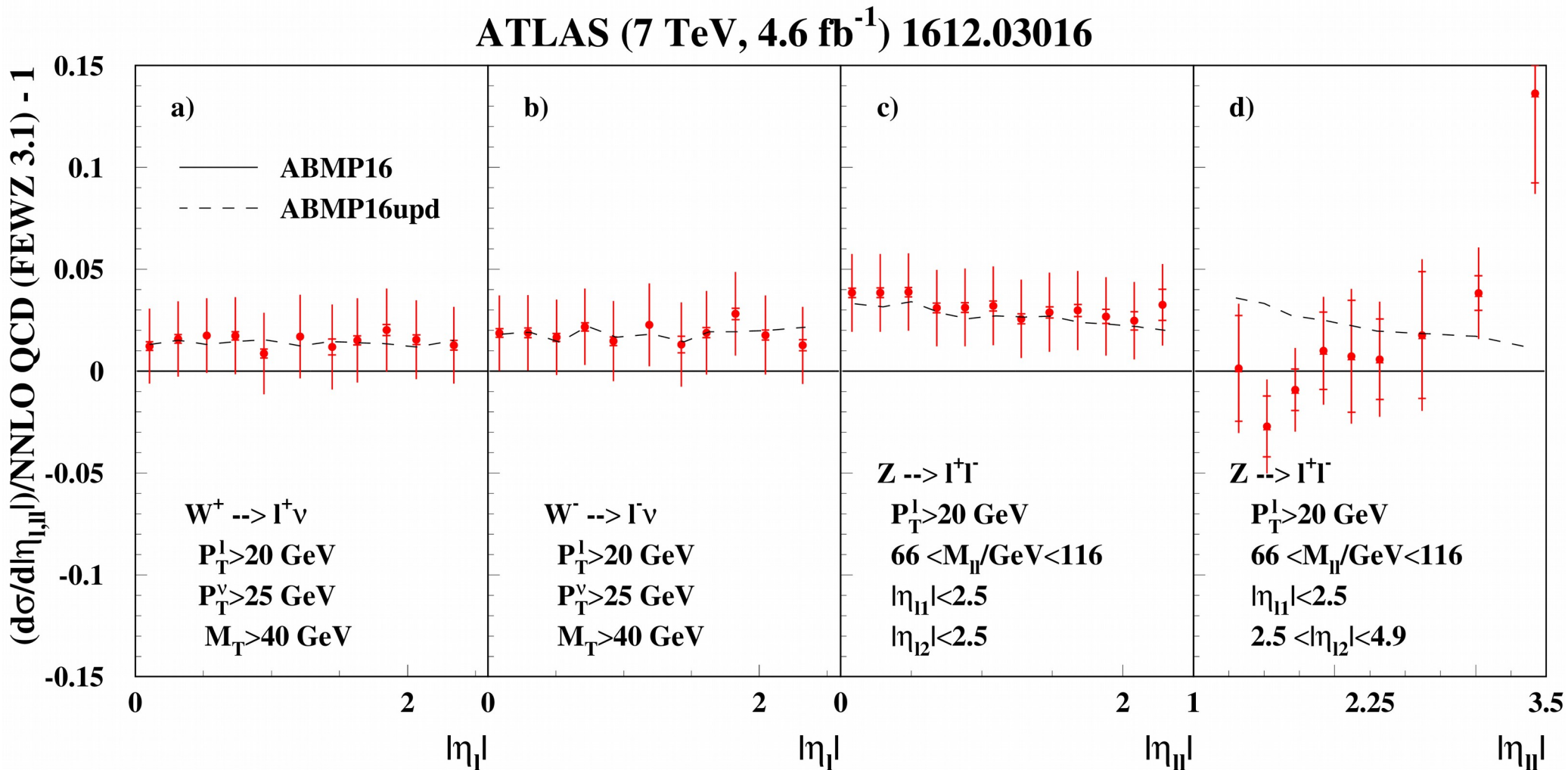
NNLO tools' benchmarking



The bands display an integration accuracy obtained with $O(\text{month})$ of the wall time

- The FEWZ predictions somewhat overshoot the data at 7 TeV, while the DYNNLO ones go lower and are in better agreement with the measurements
- At 8 TeV the tendency is different: The FEWZ predictions somewhat undershoot the data and the DYNNLO ones go essentially lower
- FEWZ predictions demonstrate better overall agreement with the data therefore this tool is routinely used in the fit

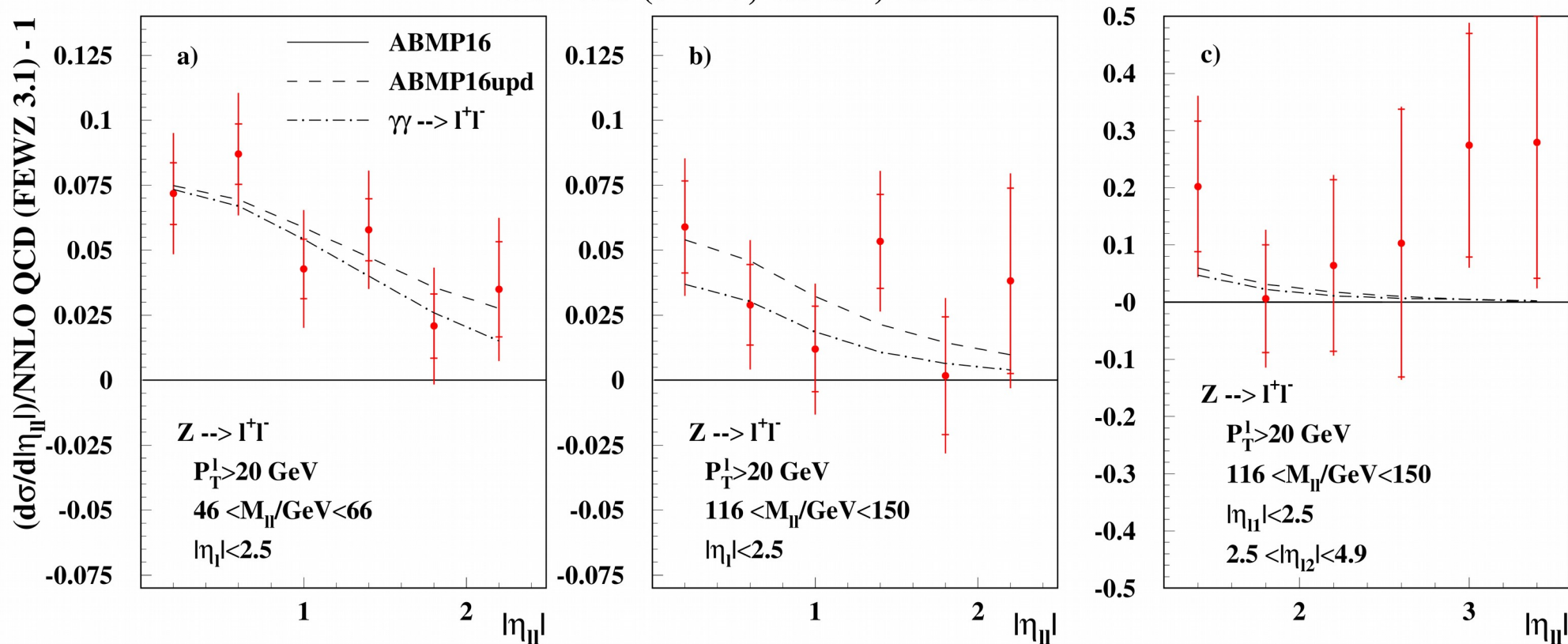
W and Z 7-TeV ATLAS data in ABM fit



Data are well accommodated in general; forward Z-boson data have particular trend, however, χ^2 is also not bad due to large errors

Non-resonant DY 7-TeV ATLAS data in ABM fit

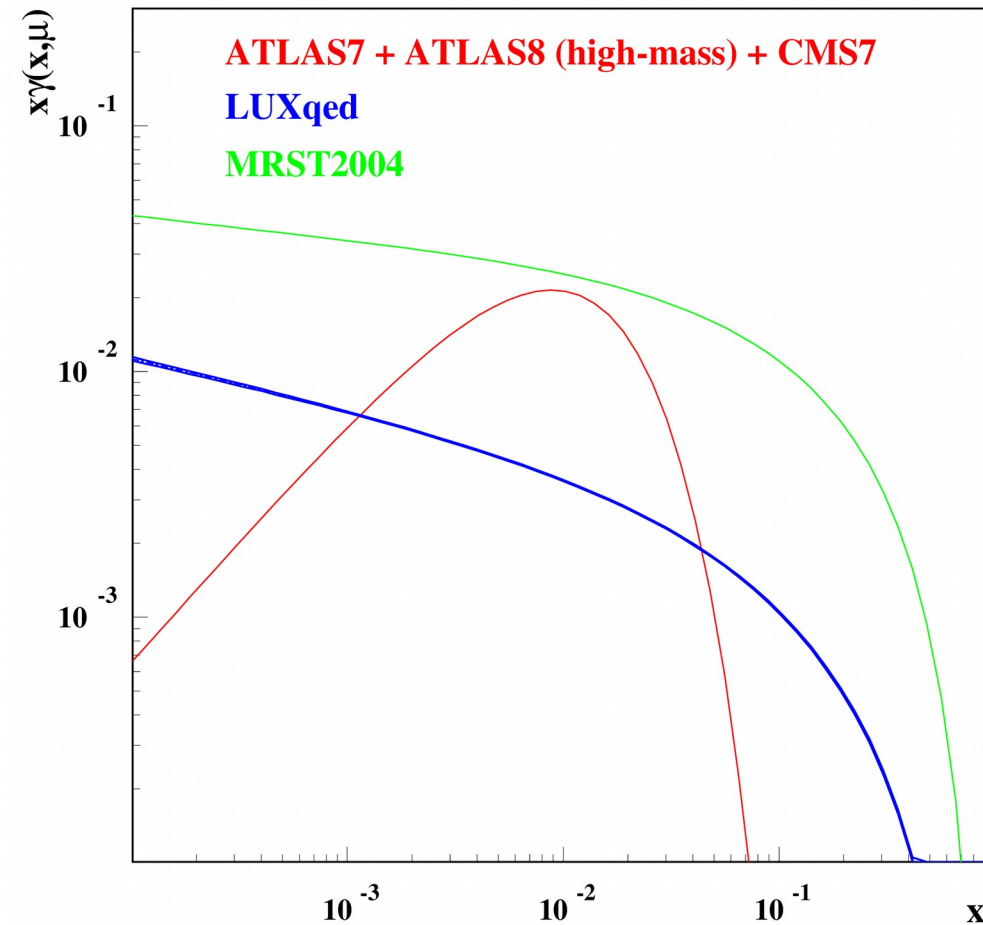
ATLAS (7 TeV, 4.6 fb⁻¹) 1612.03016



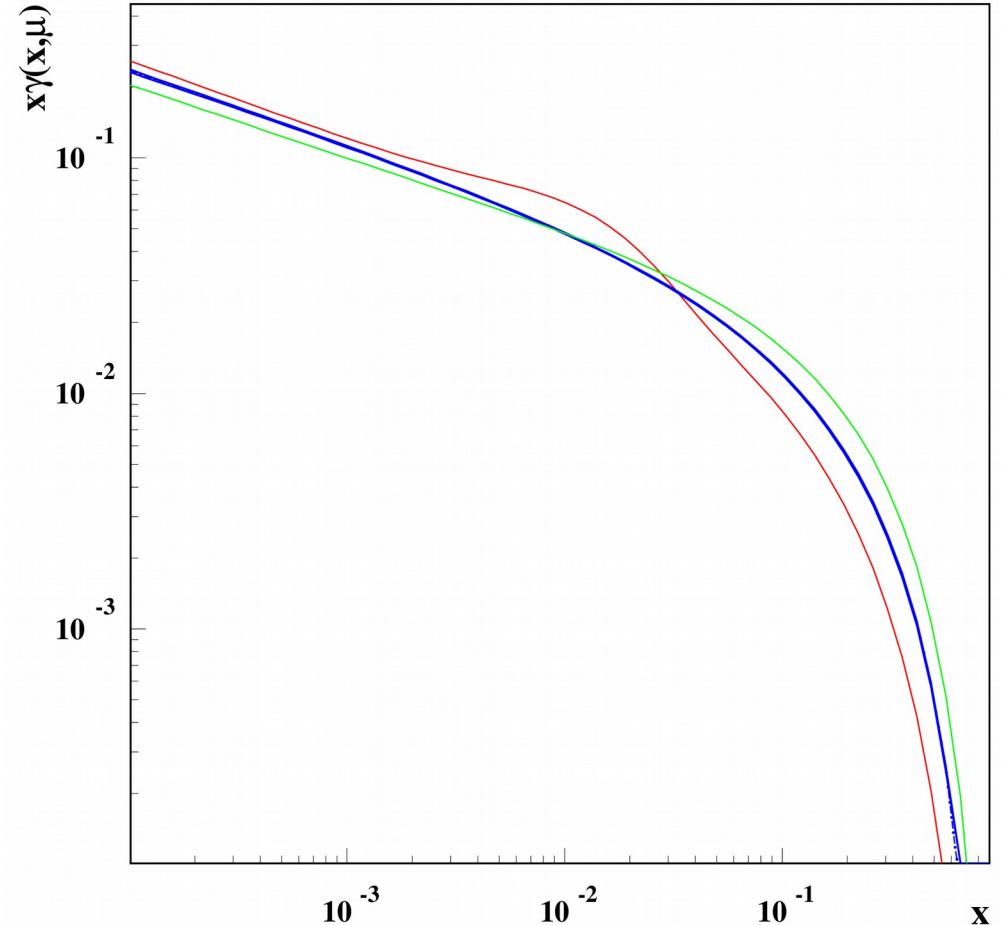
- The data can be well accommodated into the fit, the total χ^2/NDP for W, Z and $Z\gamma^*$ data is 68/61
- Account of the photon-photon contribution (in LO) improves agreement → photon distribution can be extracted from the data

Photon PDF fitted to the DY data

$\mu=3 \text{ GeV}$



$\mu=100 \text{ GeV}$



Data set	χ^2/NDP
ATLAS7 - 1612.03016	68/61
ATLAS8 (high-mass) – 1606.01736	192/132
CMS7 – 1310.7291	59/48

Quite different evolution input for the available photon distributions. Reduces at large scales, however still sensitive to the quark distributions (cf. PDF4LHC issue in LUXqed)

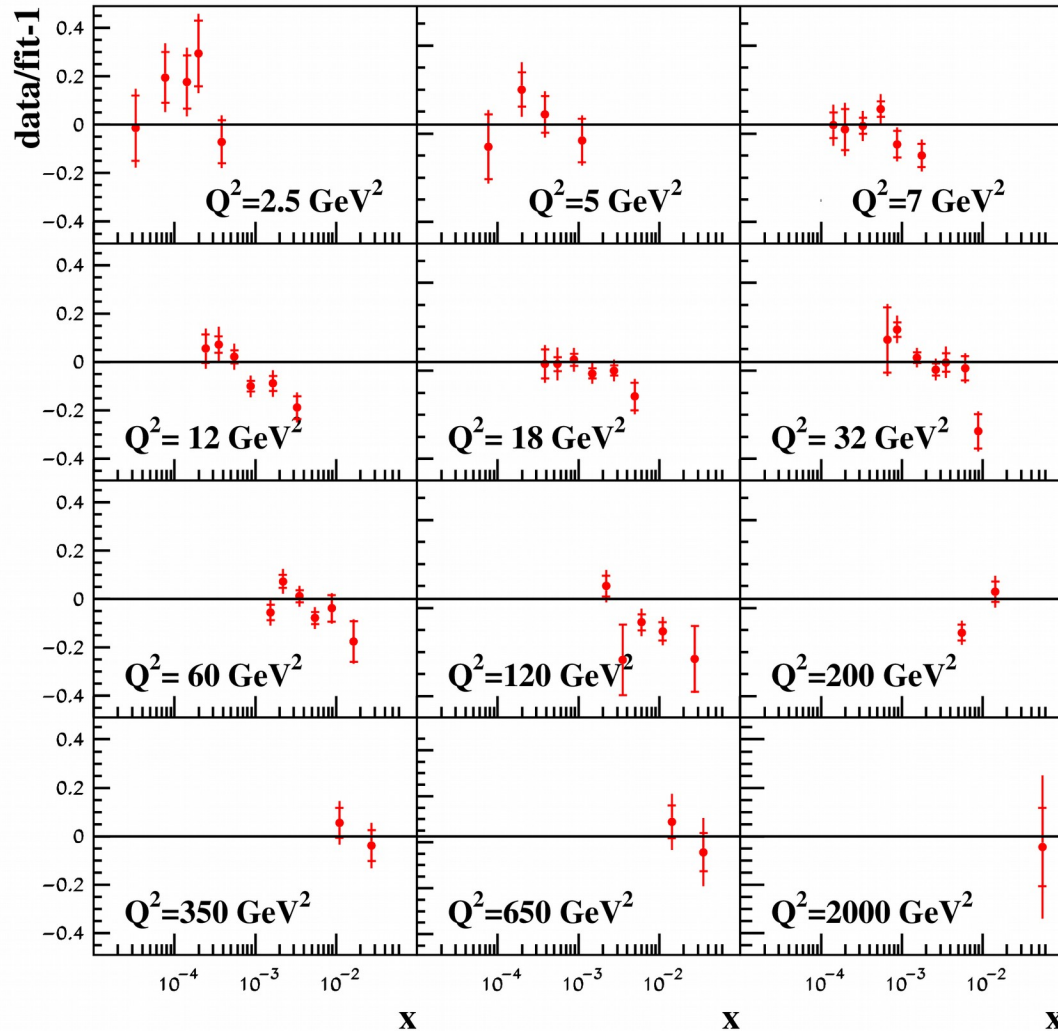
Manohar, Nason, Salam, Zanderighi hep-ph/1708.01256

The (quasi)-elastic contribution is not considered – conceptual difference with LUXqed

HERA charm data and m_c

H1, ZEUS EPJC 78, 473 (2018)

HERA I+II (ep \rightarrow e charm X)



Theory: FFN scheme, running mass definition

$$m_c(m_c) = 1.250 \pm 0.019 (\text{exp.}) \text{ GeV}$$

ABMP16upd

$$m_c(m_c) = 1.252 \pm 0.018 (\text{exp.}) \text{ GeV}$$

ABMP16

$$m_c(\text{pole}) \sim 1.9 \text{ GeV (NNLO)}$$

Marquard et al. PRL 114, 142002 (2015)

$$m_c(m_c) = 1.246 \pm 0.023 (\text{h.o.}) \text{ GeV NNLO}$$

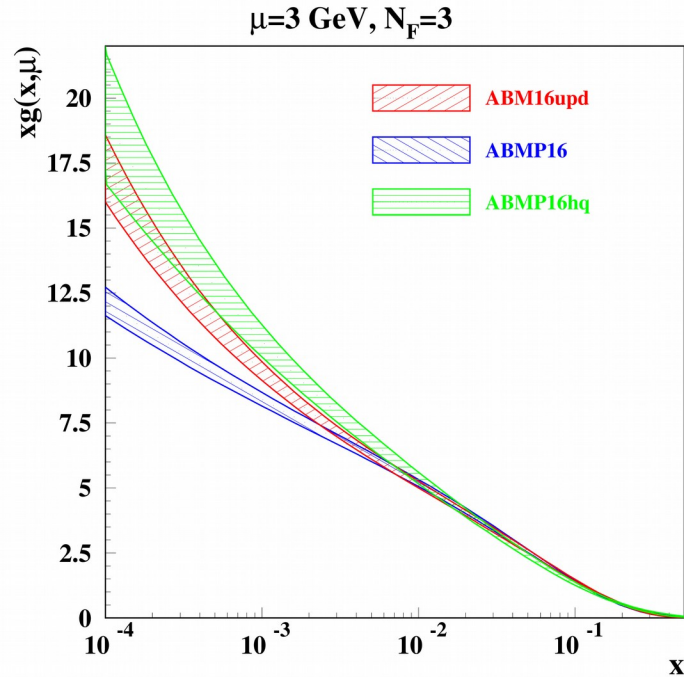
Kiyo, Mishima, Sumino PLB 752, 122 (2016)

$$m_c(m_c) = 1.279 \pm 0.008 \text{ GeV}$$

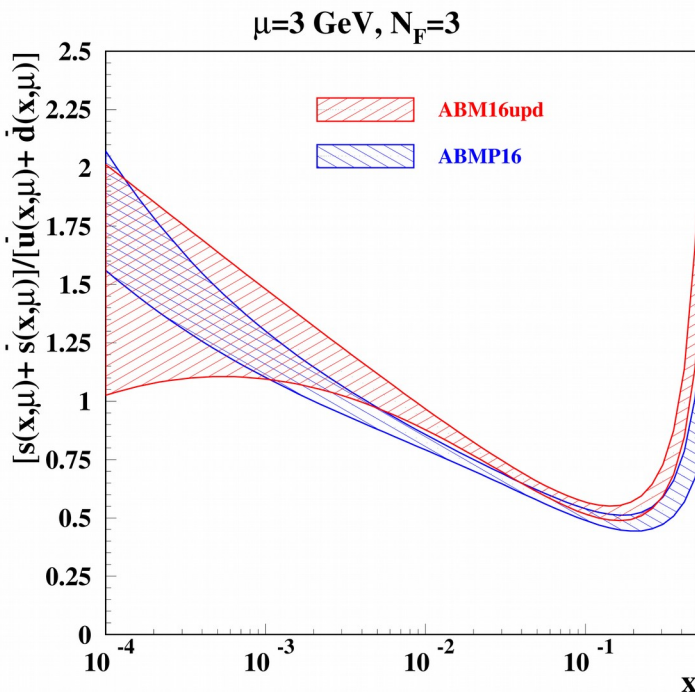
Kühn, LoopsLegs2018

Good consistency with the earlier results and other determinations \rightarrow further confirmation of the FFN scheme relevance for the HERA kinematics

Gluon and strange PDF updated

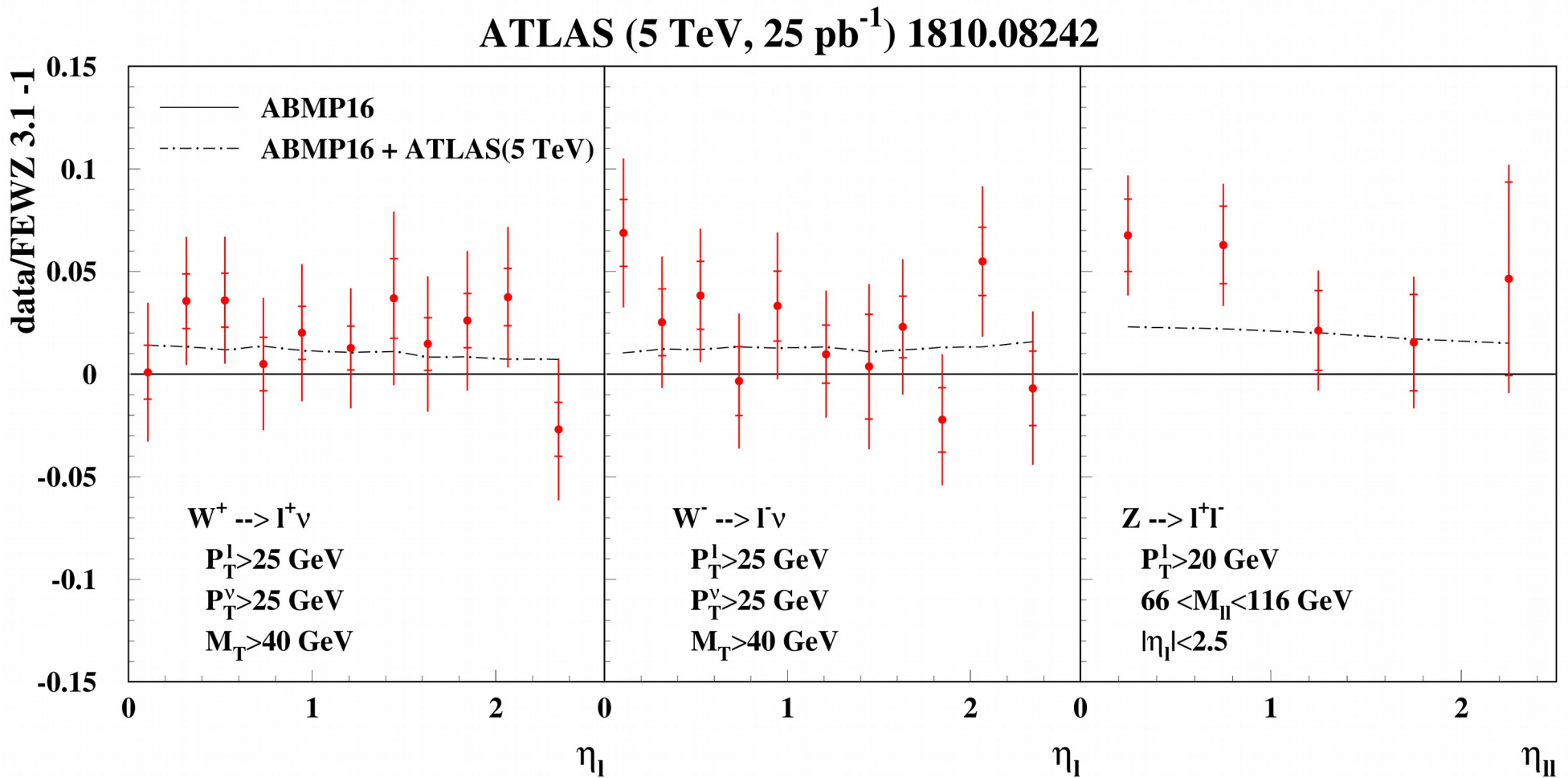


- Gluon goes higher, mainly due to more stringent cut on Q^2 (impact of the power corrections, resummations, etc. is reduced)
- Updated charm/beauty data are consistent with such an enhancement



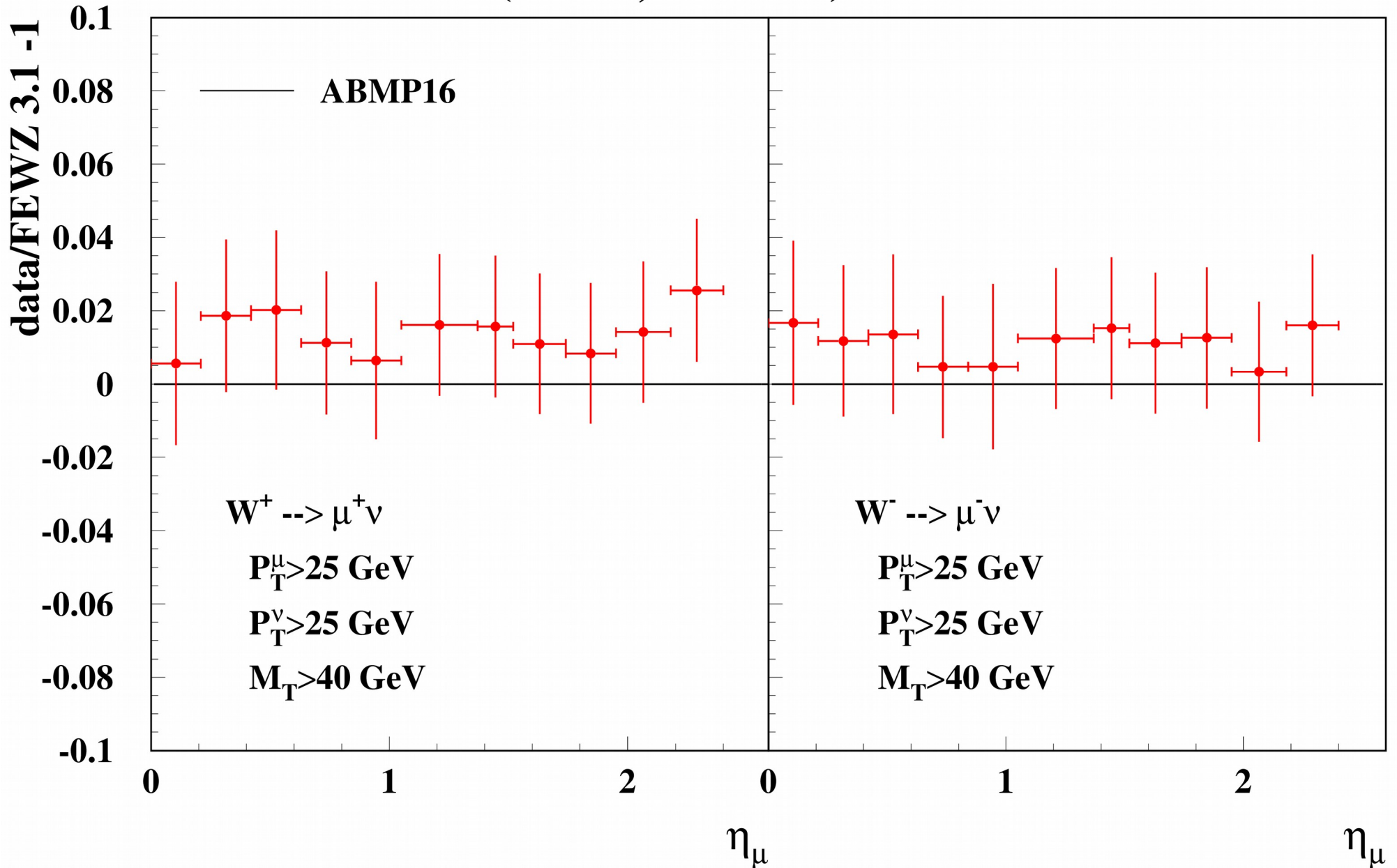
- Strange sea suppression factor goes lower at small x , consistent with 1 within errors
- At moderate x the strange sea is still suppressed, although integral suppression factor $\kappa_s(20 \text{ GeV}^2)=0.71(3)$, a little larger than $0.66(3)$ for ABMP16 fit

DY: impact of the recent data



PRELIMINARY: Uncertainty correlations are not taken into account (still unpublished); smaller impact on fit is expected when they are included

ATLAS (8 TeV, 20.2 fb⁻¹) 1904.05631



Uncertainty correlations are still unpublished

Summary and outlook

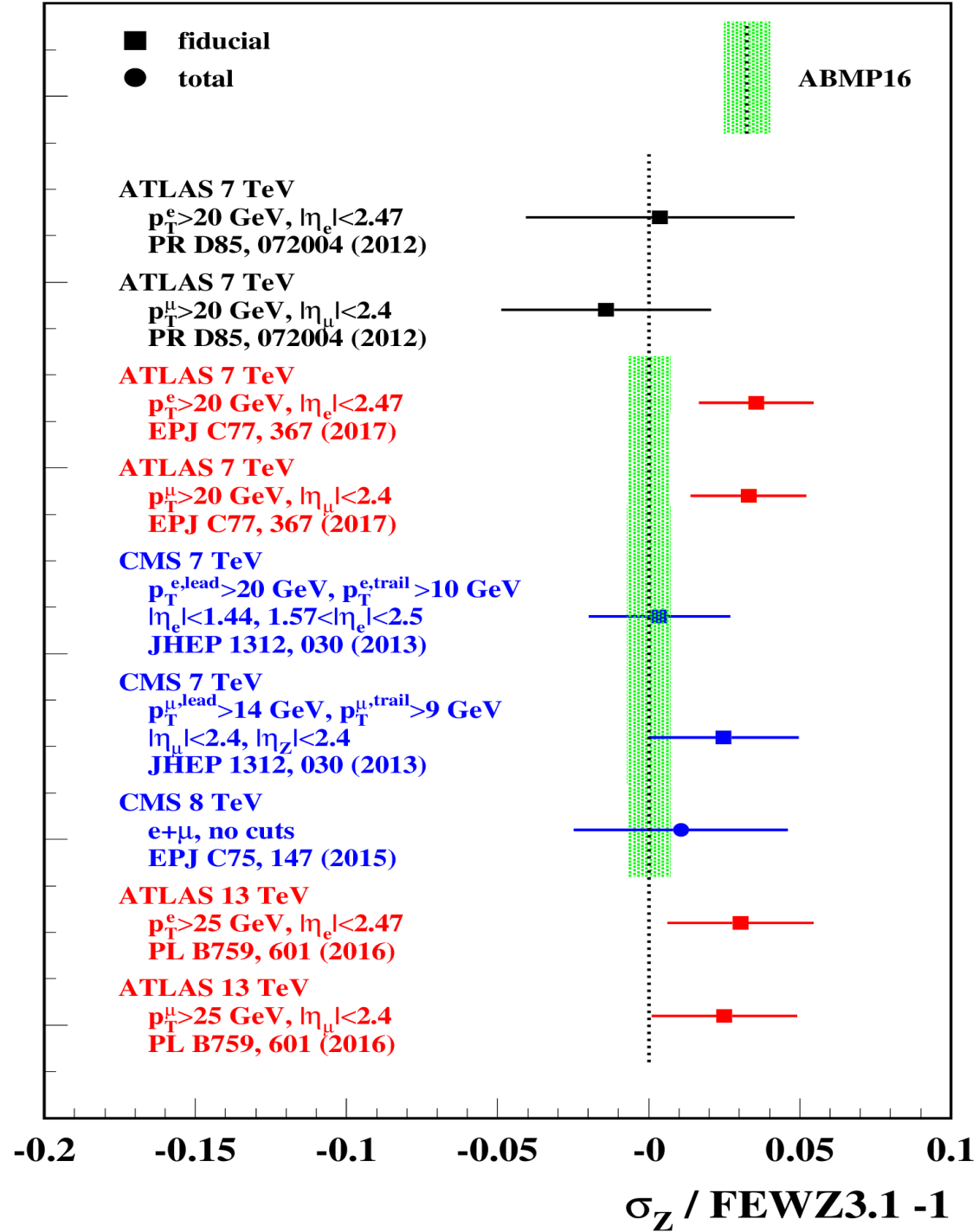
- First non-resonant ATLAS and CMS DY data have been included into ABM fit
 - QED evolution is implemented
 - smooth accommodation of the ATLAS7 ($W, Z/\gamma^*$), ATLAS8(γ^*) (high mass), CMS7(Z/γ^*) with account of the photon-photon contribution (NLO EW still has to be included)
 - first results on the photon distribution fitted to the DY data obtained
- More Z/γ^* data are being processed:

ATLAS at 8 TeV	1710.05167
ATLAS at 7 TeV	1305.4192 (high mass)
	1404.1212 (low mass)
CMS at 8 TeV	1412.1115

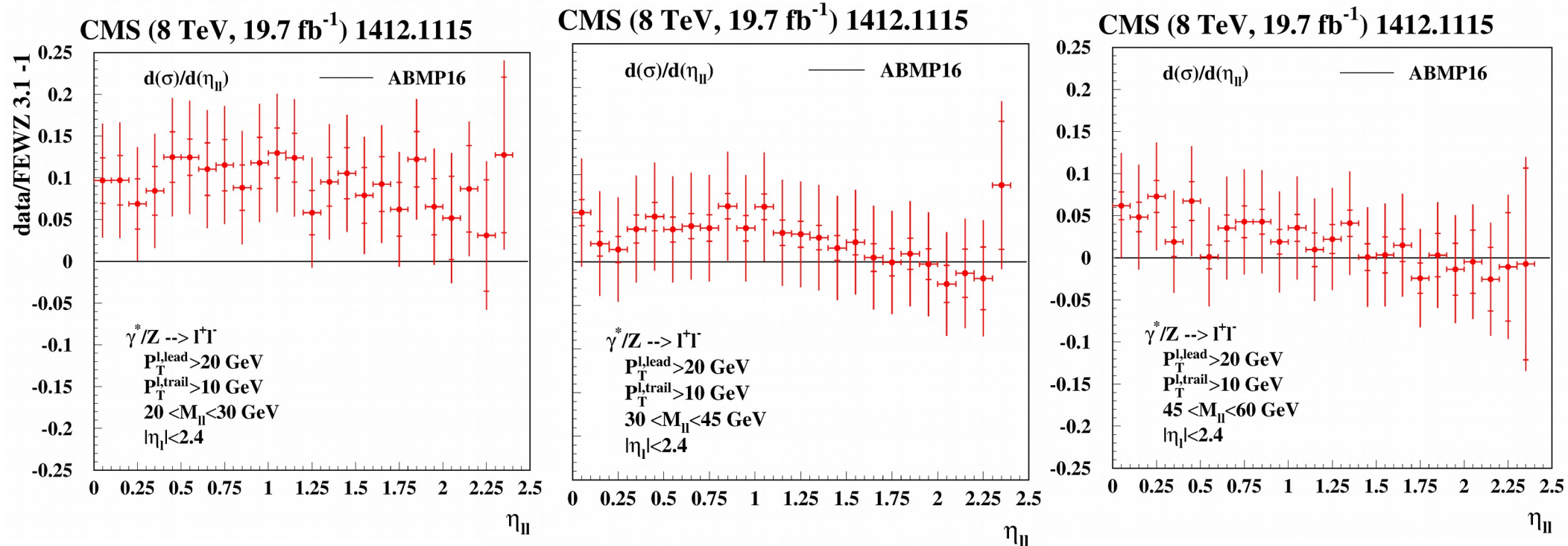
 - better constraint on photon distribution is expected
- W and Z Atlas at 5 and 8 TeV can be quickly included into the fit, when the correlation matrices are provided

EXTRAS

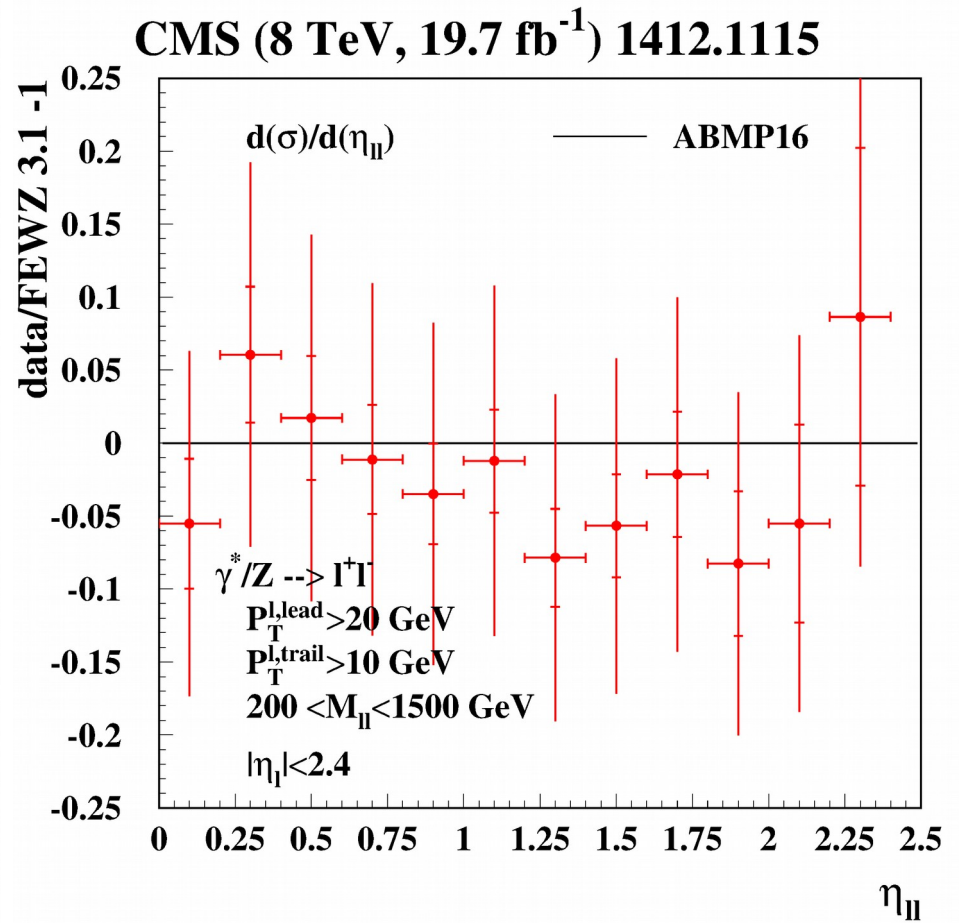
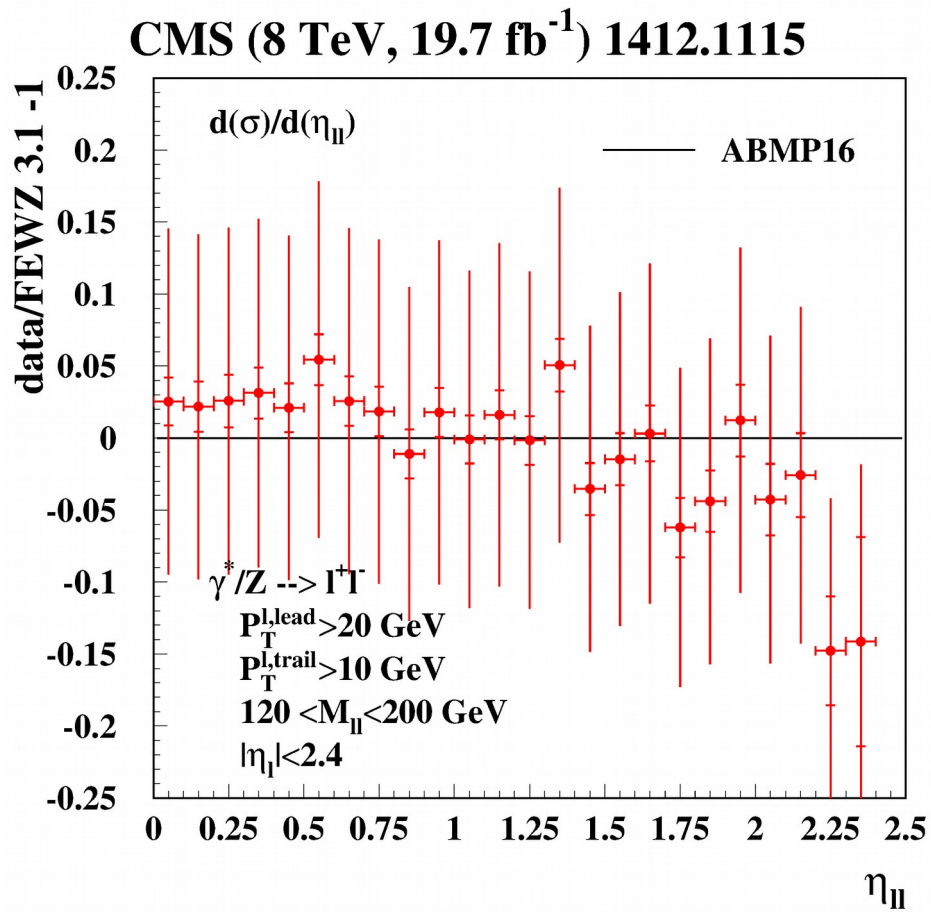
$$Z \Rightarrow l^+ l^-$$



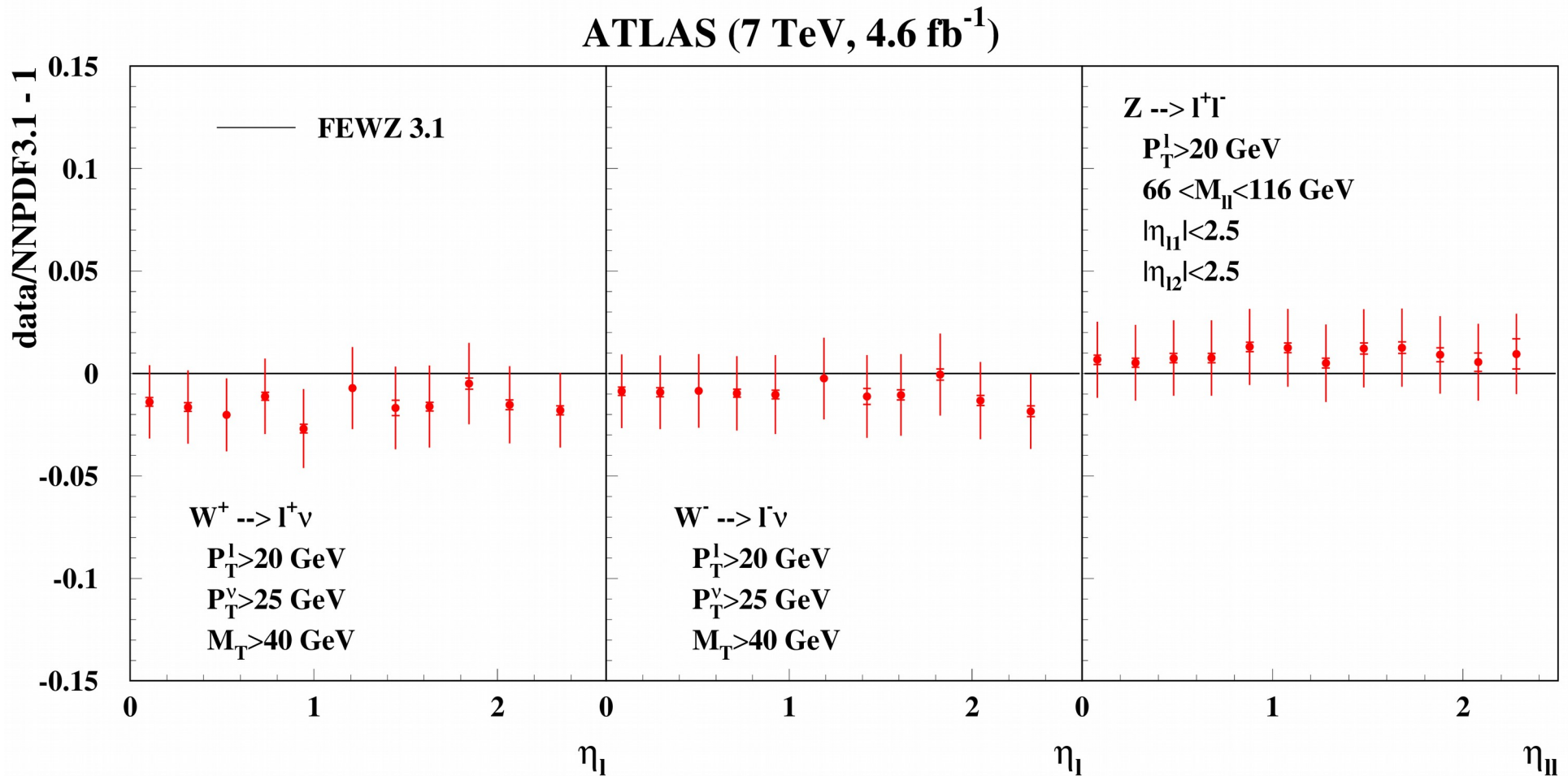
DY: towards double differential distributions



- Reasonable agreement with the previous fit predictions
- Complimentary constraint on PDFs → improved quark disentangling
- Other CMS and ATLAS data in progress; the bottleneck is NNLO computations with the fiducial-volume cuts



Closure test of the NNPDF3.1 fit



- Different trend for W and Z data $\Rightarrow \chi^2/\text{NDP} = 400/34$; problems with the flavor disentangling
- Suppressed (fitted) charm distribution requires corresponding enhancement of strangeness sur to constraint from W data

